Magnetic pulse welding of dissimilar aluminum-copper joints: Impact of downscaling on weldability

J. Jüngst[1,*], M. Graß[1], S. Böhm[1]

[1] Department for Cutting and Joining Manufacturing Processes Division of Welding Technology, University of Kassel, Germany
*Corresponding author. Email: j.juengst@uni-kassel.de

Abstract

Due to the higher specific electrical conductivity (conductivity/weight) of aluminum compared to copper and the associated lightweight potential, the electrical industry is moving towards current-conducting components made of aluminum. However, the use of aluminum is associated with a necessity for hybrid aluminum-copper joints, due to space limitations as well as purchased components are often made of copper. Furthermore, it can be observed that numerous flat conductors, such as those used in DC and asynchronous motors, are only a few millimeters wide. Due to the rapidly growing market for electric vehicles, an increasing demand for aluminum-copper dissimilar joints with small dimensions is consequently to be expected.

In contrast to conventional fusion welding processes, magnetic pulse welding (MPW) is suitable for joining aluminum-copper dissimilar joints, due to the minimization of brittle intermetallic phases. This is attributed to the low energy input, which is applied as the movement of mass to fabricate a material continuous joint.

It is known that MPW reaches its process limits when the dimensions of the joining partners decreases due to the minimization of effective eddy currents. However, these limits are still insufficiently researched. Consequently, this investigation is intended to reveal the process limitations of MPW with regard to the joining partner dimensions. For this purpose, various geometries are evaluated with regard to their weldability and the resulting microstructural, mechanical and electrical properties.

Keywords

magnetic pulse welding, aluminum-copper dissimilar joints, joining partner dimension

1 Introduction

Due to the increasing electrification of vehicles and the associated high number of electrical contacts, these are becoming increasingly important. In Germany the number of newly registered electric cars increased by almost 270% between 2020 and 2023. The market only declined in 2024 due to the end of state funding for electric cars at the end of 2023. However, it can be assumed that the market will recover from this year onwards. In January 2025, an increase of 53.5% in electric car registrations was observed compared to January 2024. Strong global demand for electric cars can also be observed. Over 14.8 million new electric cars were registered worldwide in 2023. (Statista 2025a, 2025b)
Flat electrical conductors, as exemplified by those found in direct current (DC) and asynchronous motors, as well as in battery packs, are experiencing a marked increase in importance. In the context of the EU's goal of climate neutrality by 2050 (Europäische Kommission 2024), the concept of lightweight construction is also gaining in importance in the automotive sector. The potential for lightweight construction in electrical applications is given by the partial substitution of copper by aluminum due to its higher specific electrical conductivity in current-conducting components (Graß and Böhm 2023). Furthermore, the industry continues to strive the replacement of copper flat conductors with aluminum flat conductors due to the enormous cost savings of more than 80% (boerse.de 2025a, 2025b).
However, complete material substitution is not possible because of the design of purchased power electronic components made of copper or installation space restrictions that require the use of copper. This results in the necessity of aluminum-copper dissimilar joints. Compared to conventional fusion welding processes, magnetic pulse welding (MPW) is suitable for joining dissimilar joints, as the joining partners are only thermally impacted locally in the joint area. As a result, intermetallic phases are significantly minimized.
Since flat electrical conductors in electric motors are only a few millimetres wide due to space restrictions, it is important to investigate how reduced joining partner dimensions affect the weldability of MPW.

2 Experimental Setup

2.1 Magnetic Pulse Welding

The Blue Wave PS48-16 MPW system from the manufacturer PSTproducts GmbH was used for the experiments described in this publication. The six capacitors of the MPW system can store up to 48 kJ at a maximum charging voltage of 16 kV. The active area of the flat coil used is characterized by its coil length of 160 mm and width of 10 mm. During the welding process, a high-current pulse generated by the capacitors flows through the flat coil, creating a magnetic field surrounding the active area of the coil radially. The magnetic field in turn causes the induction of eddy currents in the first joining partner (flyer) arranged above it (shown in Figure 2(b) in Watanabe and Kumai 2009). The principle of mutual induction causes the formation of a secondary magnetic field around the flyer, which is directed in the opposite direction to the primary magnetic field of the coil. The resulting electromagnetic

force (Lorentz force) accelerates the flyer in the direction of the second joining partner (parent). The necessary acceleration distance is set up using suitable spacers. The flyer plate then collides with the parent plate at high speed and conducts a rolling movement, which is characteristic for MPW (shown in Figure 46 in Mori et al. 2013; Hahn et al. 2016)). Due to the high impact speed (several hundred m/s), or more precisely, due to the high impact pressure (up to a few thousand MPa) of the joining partners, parts of the boundary layers of the joining partners are plastified and ejected out of the closing gap between Flyer and Target (Jetting effect). Finally a metallic bond occurs (Chaturvedi and Arungalai Vendan 2021; Mori et al. 2013).

2.2 Materials, specimen dimensions and welding parameters

The aim of this publication is to determine the weldability of aluminum-copper dissimilar joints using varying joint partner widths. For this purpose, sheets made of the aluminum alloy AA 1050A (flyer plate) and the copper alloy Cu-ETP (parent plate) with the mechanical properties shown in **Table 1** were used. The sheet thickness for both alloys is 1 mm.

Alloy	Tensile strength [MPa]	Fracture strain [%]
AA 1050A	120,22	5,13
Cu-ETP	269	32

Table 1: *Mechanical properties of the used alloys*

To identify the lower process limit, the width of the joining partner was reduced iteratively in 1 mm steps from 15 mm on. Furthermore, the remaining framework conditions of the welding configuration were kept constant. A schematic representation of the welding configuration is shown in **Figure 1**. For the investigations carried out in this paper an acceleration distance of 1 mm, a discharge current of 482,7 kA and a constant overlap length of 20 mm was used. With the system technology used for these investigations, the used discharge current still represents the mechanical load limit of the flat coil used. A further increase in the discharge current is therefore not recommended.

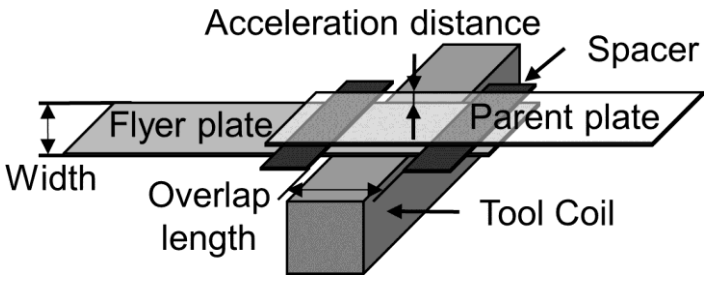

Figure 1: *Schematic overview of the welding configuration*

2.3 Electrical Characterization

The MR200C micro-ohmmeter from Schuetz, which uses the Kelvin four-wire resistance measurement **(Figure 2**), is used for the electrical characterization of the welded specimens.

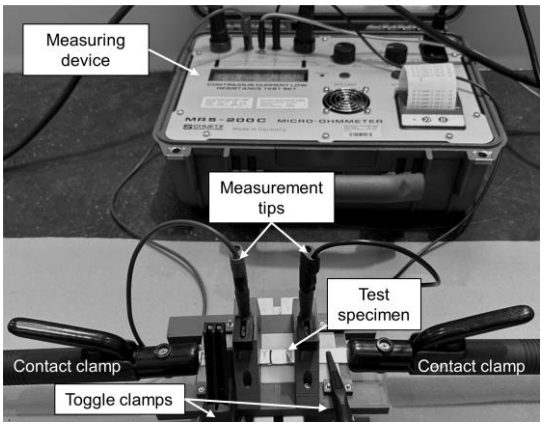

Figure 2: *Resistance measurement setup*

When positioning the specimen in the resistance measurement setup shown in **Figure 2,** the weld seam has to be centered between the two measurement tips. The two measurement tips are then lowered onto the specimen surface. Based on (Graß et al. 2024), a current of 50 A is then applied allowing the local voltage to be measured with high resistance via the measurement tips. The resistance of the joint is then determined from the voltage difference between the measurement tips according to **Eq. (1)**.

$$R_{MPW} = \frac{\Delta U}{I} \tag{1}$$

Reference measurements were also carried out to quantify the results of the electrical characterization. To reference the electrical resistance values, the aluminum and copper base materials were also electrically tested for each joint partner width. The reference resistance of the joint was then calculated according to **Eq.(2)**. Finally, the electrical resistance of the specimens was also normalized to its reference condition for graphical representation.

$$R_{ref} = \frac{1}{2}(R_{Al} + R_{Cu}) \tag{2}$$

2.4 Mechanical Characterization

The welded specimens were tested and evaluated mechanically in the quasi-static shear tensile test with a universal tensile testing machine (Z100, ZwickRoell GmbH & Co. KG) at 5 mm/min. A specimen that failed in the aluminum base material was assumed to be OK. In order to be able to quantify the results of the mechanical characterization adequately, reference measurements were carried out. The aluminum sheet represents the reference state

for the mechanical tests, as this is the weakest joining partner in terms of tensile strength. Based on a reference tensile specimen, the maximum tolerable force per joint partner width was calculated by multiplying it by the cross-sectional area. The maximum tolerable forces of the specimens were normalized to their respective reference condition for graphical representation.

2.5 Weld Seam Analysis

To determine the weld area on the parent plate (Cu sheet) by using optical macroscopy (Leica Z16), the flyer plate (Al sheet) was first dissolved in 10 % sodium hydroxide solution for 24 hours. The weld seam area can then be recognized as a dark ellipse on the copper sheet.
For microstructural analysis of the specimens, they were analysed metallographically. For this purpose, the specimens were embedded in a resin compound, ground and polished. Scanning electron microscope (SEM, Zeiss ULTRA PLUS) and energy-dispersive X-ray spectroscopy (EDS, Bruker 6|60) examinations subsequently allow statements to be made about the weld seam characteristics in the interfaces of the joining partners.

3 Results

When looking at **Figure 3,** it can be seen that the normalized electrical resistance of 15 mm to 9 mm joint partner width is at a similarly good level. Due to the overlap joint design, the magnetic pulse welded specimens have a lower resistance than the reference sheets. As a result, the flat conductor in the weld area has a larger cross-section than the reference sheet. Just like the electrical resistance, the mechanical behavior of the samples in the widths of 15 mm to 9 mm can be evaluated as positive. These specimens completely failed in the aluminum base material in the quasi-static shear tensile test. Due to the overlap joint of the welded specimens, which results in a complex stress situation, the maximum tolerable force is lower than that of the aluminum base material **(Figure 3).**

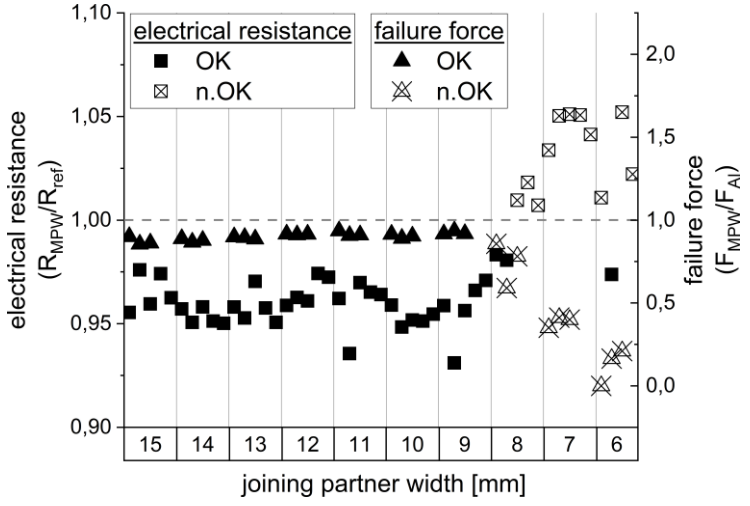

Figure 3: *Standardized electrical resistance and failure force of the specimens*

Joining partner widths of 8 mm and less are to be rated as not OK, as they either have bad electrical or mechanical properties, or both. An intended joint of 5 mm wide sheets is not shown in **Figure 3** as it could not be welded. Even increasing the discharge current to 497,2 kA did not result in a welded joint.

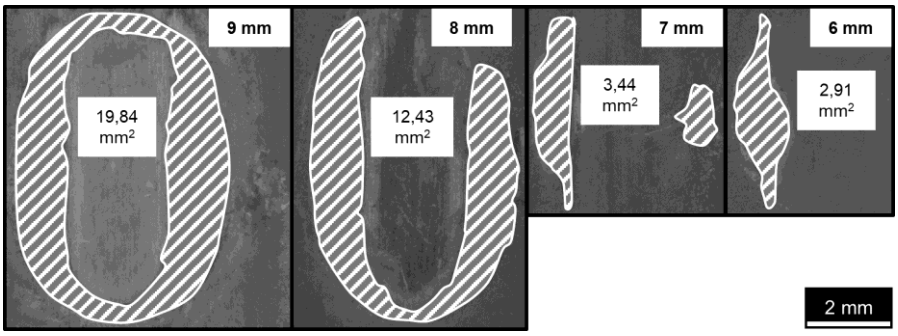

Figure 4: *Macroscopic comparison of the welded areas of the samples in widths of 6 mm to 9 mm*

The macroscopic images confirm a reduction in the weld joint at sheet widths of 8 mm and less. **Figure 4** shows that no elliptical weld seam typical of the MPW is formed. A further reduction in the joining partner width results even more clearly in a reduced welding area.

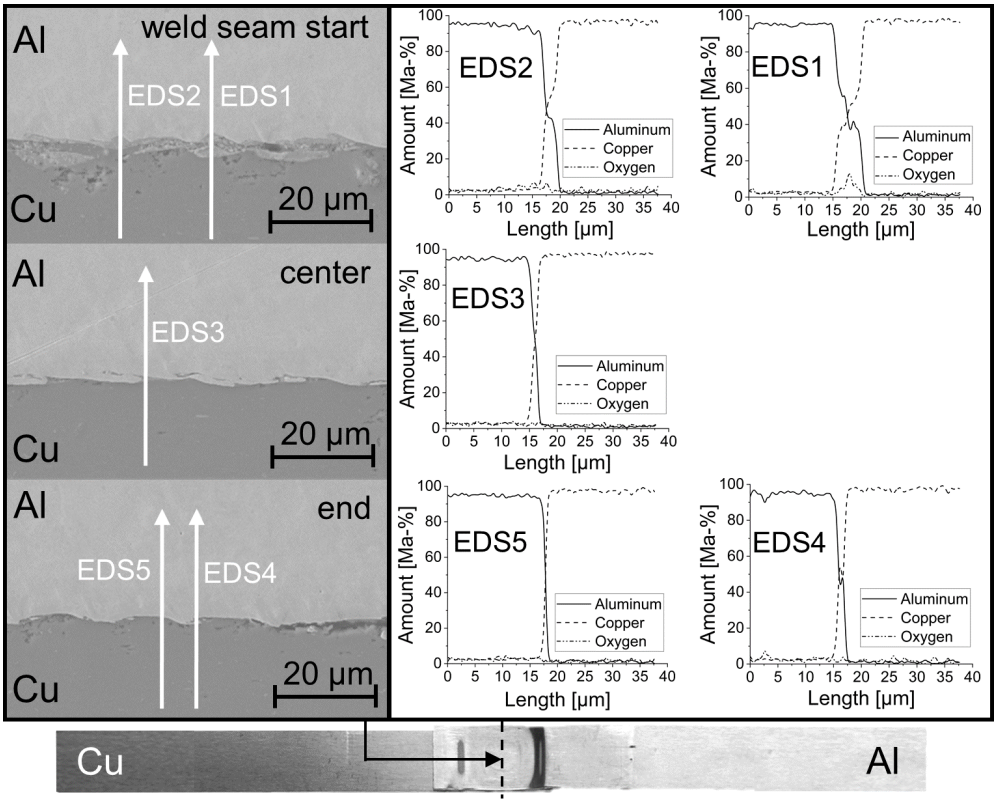

Figure 5: *SE2 images and EDS analysis of the weld seam of the 15 mm wide specimen with an accelerating voltage of 16 kV and a working distance of 10 mm*

The SEM images in **Figure 5** show typical interface characteristics of an MPW weld. There are clearly differentiated-looking phases before the start of the weld seam. These show an enrichment of oxygen in EDS 1. A trapped jet can be assumed in this area, which typically rolls over locally during the welding process. The weld seam center also shows typical characteristics of an MPW welded seam in the form of wave formation in the interface of the joining partners. The EDS analyses also show the typical characteristic of the interface for the MPW that the width of the interface decreases continuously towards the end of the weld seam.

4 Conclusion and Outlook

In this publication, the assumption of the process limit for MPW depending on the minimum weldable sheet width was confirmed. A substrate combination of AA 1050A and Cu-ETP with a thickness of 1 mm was used for this investigation. The MPW process limit could be determined with the used system technology at a minimum sheet width of 6 mm. However, superior electrical and mechanical properties could only be realized with 9 mm or wider joining partners. The associated welding area also confirms the determined MPW process limit. A complete ellipse of the weld seam is only achieved with a joining partner width of 9 mm or greater. In view of the rapidly decreasing welding area with a joining partner width of 8 mm and below and the small welding area with a joining partner width of 6 mm, it seems logical that a joining partner width of 5 mm no longer permits welding.
Future investigations with a more powerful system technology would have to clarify whether a significant increase in the discharge energy and, thus, a significant increase in the current flowing through the coil would allow a further minimization of the joint partner width. Furthermore, it would be of interest to investigate the influence of the surface modification of the joining partners on the possibility of further minimizing the joining partner width in relation to the material combination used in this publication. Further investigations of different welding configurations, which have a controlled influence on the rolling movement, e.g. by previously deformed joining partners or a one-sided positioning, would have to be analyzed with regard to their influence on the downscaling.

5 Acknowledgment

The shown results were achieved in the project “Mehrfachkontaktierung von Statorwicklungen eines elektrischen Antriebs durch Magnetimpulsschweißen (MULTI-KON)” (reference IGF 01IF23420N), which is supervised by the Forschungsvereinigung Schweißen und verwandte Verfahren e.V. of the German Welding Society and funded by the German Aerospace Center (DLR) by means of the Federal Ministry for Economic Affairs and Climate Action (BMWK) on the basis of a decision by the German Bundestag.

References

boerse.de (2025a): Aluminium EUR | Euro Aluminiumpreis aktuell | Euro Aluminiumkurs heute - boerse.de. Available online at https://www.boerse.de/rohstoffe/Aluminiumpreis/XC0009677839, updated on 3/5/2025, checked on 3/5/2025.

boerse.de (2025b): Kupfer EUR | Euro Kupferpreis aktuell | Euro Kupferkurs heute - boerse.de. Available online at https://www.boerse.de/rohstoffe/Kupferpreis/XC0005705501, updated on 3/5/2025, checked on 3/5/2025.

Chaturvedi, Mukti; Arungalai Vendan, S. (2021): Magnetic Pulse Welding and Design. In Mukti Chaturvedi, S. Arungalai Vendan (Eds.): Advanced Welding Techniques. Holistic View with Design Perspectives. 1st ed. 2021. Singapore: Springer Singapore; Imprint Springer, pp. 167–197.

Europäische Kommission (2024): Neues Ziel für 2040: Empfehlung zur Verwirklichung der Klimaneutralität bis 2050. Available online at https://commission.europa.eu/news/recommendation-2040-target-reach-climate-neutrality-2050-2024-02-06_de, updated on 2/6/2024, checked on 3/5/2025.

Graß, M.; Böhm, S. (2023): Einsatz des Magnetimpulsschweißens für elektrisch beanspruchte Litze-Ableiter-Verbindungen. In DVS Media GmbH (Ed.): DVS Congress 2023. Große Schweißtechnische Tagung DVS CAMPUS. Ausführliche Manuskripte auf USB-Card, vol. 389. DVS Congress 2023. Essen, Deutschland, 11.09.2023-14.09.2023. Deutscher Verband für Schweißen und verwandte Verfahren e.V. (DVS). Düsseldorf: DVS Media GmbH, pp. 130–136.

Hahn, Marlon; Weddeling, Christian; Lueg-Althoff, Joern; Tekkaya, A. Erman (2016): Analytical approach for magnetic pulse welding of sheet connections. In *Journal of Materials Processing Technology* 230, pp. 131–142. DOI: 10.1016/j.jmatprotec.2015.11.021.

Mori, Ken-ichiro; Bay, Niels; Fratini, Livan; Micari, Fabrizio; Tekkaya, A. Erman (2013): Joining by plastic deformation. In *CIRP Annals* 62 (2), pp. 673–694. DOI: 10.1016/j.cirp.2013.05.004.

Statista (2025a): Anteil von Elektroautos in Deutschland 2025 | Statista. Available online at https://de.statista.com/statistik/daten/studie/784986/umfrage/marktanteil-von-elektrofahrzeugen-in-deutschland/, updated on 3/5/2025, checked on 3/5/2025.

Statista (2025b): Zulassungszahlen von Elektroautos 2025 | Statista. Available online at https://de.statista.com/statistik/daten/studie/244000/umfrage/neuzulassungen-von-elektroautos-in-deutschland/, updated on 3/5/2025, checked on 3/5/2025.

Watanabe, Mitsuhiro; Kumai, Shinji (2009): Interfacial Morphology of Magnetic Pulse Welded Aluminum/Aluminum and Copper/Copper Lap Joints. In *Mater. Trans.* 50 (2), pp. 286–292. DOI: 10.2320/matertrans.L-MRA2008843.

Graß, M.; Sommer, N.; Böhm, S. (2024): Enabling magnetic pulse welding for dissimilar tubular arrester cable joints. In *Weld World* 68 (7), pp. 1837–1852. DOI: 10.1007/s40194-024-01760-2.